

Modulation cancellation method in laser spectroscopy

V. Spagnolo · L. Dong · A.A. Kosterev · D. Thomazy ·
J.H. Doty III · F.K. Tittel

Received: 28 February 2011 / Published online: 9 April 2011
© Springer-Verlag 2011

Abstract A novel spectroscopic technique based on modulation spectroscopy with two excitation sources and quartz enhanced photoacoustic spectroscopy is described. We demonstrated two potential applications of this detection technique. First, we investigated the measurement of small temperature differences in a gas mixture. In this case, a sensitivity of 30 mK in 17 sec was achieved for a C_2H_2/N_2 gas mixture with a 0.5% C_2H_2 concentration. Second, we demonstrated the detection of broadband absorbing chemical species, for which we selected hydrazine as the target molecule and achieved a detection limit of ~ 1 part per million in 1 sec. In both cases, the measurements were performed with near-IR laser diodes and overtone transitions.

A widely used technique for spectroscopic detection of absorption, scattering, laser induced fluorescence, and related optical phenomena is modulation spectroscopy. In this technique, the excitation radiation (usually laser radiation) is modulated at a certain frequency f , and the detector response is demodulated at the same frequency or one of its

harmonics ($2f, 3f, \dots$). The primary advantages of such an approach are the following:

- (1) Detection can be performed at a frequency where source and detector noise are minimal;
- (2) When $2f$ or higher harmonics are used in the wavelength modulation (WM) absorption spectroscopy, the baseline is efficiently suppressed (background-free detection).

The modulation cancellation method (MOCAM) is a variation of modulation spectroscopy with two excitation sources [1, 2]. The basic concept of MOCAM is that the powers and modulation phases of two lasers are adjusted to balance out the background signal which would otherwise limit the accuracy or interfere with the measurements. Possible MOCAM applications include the characterization of isotopic composition [3–5] and measurements of small temperature differences [6] in a gas mixture. In order to perform these measurements, the output powers and modulation phases of the two lasers resonant with two selected absorption lines are adjusted in such a way that the signal detected from the reference sample is zero. Then, in an appropriately designed optical configuration, the signal from the analyzed sample will be directly proportional to the deviation of the absorption line strength ratio from the reference line strength ratio. Another application for MOCAM is its use for the detection of broadband absorbers (large molecular species with congested, unresolved bands with $> 50 \text{ cm}^{-1}$ spectral width) in the presence of spectrally non-selective background absorption [7], where the background from scattered light strongly interferes with the informative signal. In this case, one of the lasers is centered on the target absorption feature, while the second source is tuned to its baseline. The two lasers can be modulated in counterphase so that no signal is detected in the absence of absorbing gas,

V. Spagnolo (✉) · L. Dong · A.A. Kosterev · D. Thomazy ·
J.H. Doty III · F.K. Tittel

Department of Electrical and Computer Engineering, Rice
University, 6100 South Main Street, Houston, TX 77005-1892,
USA
e-mail: spagnolo@fisica.uniba.it

V. Spagnolo
Dipartimento Interateneo di Fisica, Università e Politecnico
di Bari, CNR—IFN UOS BARI, Via Amendola 173, 70126 Bari,
Italy

Present address:

A.A. Kosterev
Yokogawa Corporation of America, 910 Gemini St., Houston,
TX 77058, USA

and in this way the background signal can be strongly suppressed.

MOCAM can be used in various implementations, including $2f$ WM absorption spectroscopy and amplitude modulation (AM), or WM ($1f$ or $2f$) photoacoustic spectroscopy. In this paper, we will describe two MOCAM applications in detail, the measurements of small temperature differences, and the detection of hydrazine at atmospheric pressure.

1 MOCAM for temperature measurements of a gas mixture

Several applications of analytical spectroscopy require the determination of the deviation of the ratio R of intensities of two absorption peaks with respect to the ratio in the reference sample R_{st} or for the reference conditions. In these cases, the deviation from the reference $\delta[\%]$ is expressed as

$$\delta[\%] = \frac{R - R_{st}}{R_{st}} \times 1000 \quad (1)$$

The existing spectroscopic approaches to measure δ are based on precise separate measurements of the selected absorption lines with the subsequent numerical calculation of δ . For isotopic characterization of samples, practically important values of δ range from $\sim 1\%$ to 0.1% . Making such precise measurements are extremely difficult due to small variations in pressure, laser power, and other external factors. As opposed to this approach, MOCAM relies on the *physical* cancellation of the measured sensor response if $R = R_{st}$. Two possible applications of this spectroscopic method are the characterization of the isotopic composition and temperature measurements. Since temperature measurements do not require costly gas samples of calibrated isotopic enrichment, they offer a convenient way to perform a MOCAM feasibility study. Thus, we implemented a sensor for spectroscopic measurements of small temperature differences in a gas mixture using quartz enhanced photoacoustic spectroscopy (QEPAS) as a detection technique [8, 9].

The absorption line strength S is independent of pressure and depends only on temperature. Thus, the ratio of the peak heights of two lines depends only on their (known) molecular parameters and T . The absorption line strength S at any temperature T can be expressed by [10]:

$$S(T) = S(T_0) \frac{Q(T_0)}{Q(T)} \exp\left[\frac{-hcE_r}{k} \left(\frac{1}{T} - \frac{1}{T_0}\right)\right] \times x \left(\frac{1 - \exp(-hcv/kT)}{1 - \exp(-hcv/kT_0)}\right) \quad (2)$$

where h is the Planck constant, k is the Boltzmann constant and c the speed of light. $S(T_0)$ is the line strength at refer-

ence temperature T_0 . The Q terms represent the total internal partition functions and can be computed [11]. The exponential term containing E_r (the total rotational energy of the molecular quantum state absorbing radiation) accounts for the rotational Boltzmann populations at T and T_0 . The last term accounts for stimulated emission, which at the laser frequencies and temperatures of interest, can be neglected. In taking the ratio of two nearby lines having different rotational energies, one obtains:

$$R = \frac{S_1(T_0)}{S_2(T_0)} \exp\left[\frac{-hc\Delta E}{k} \left(\frac{1}{T} - \frac{1}{T_0}\right)\right] \quad (3)$$

where ΔE is the difference in lower state energy between the two absorption lines. In a first approximation for small changes of temperature, the ratio of intensities is

$$R = const \times \exp\left(-\frac{\Delta E}{kT}\right) \quad (4)$$

Thus,

$$\frac{dT}{T} = \frac{dR}{R} \frac{kT}{\Delta E} \quad (5)$$

where T is approximately constant; hence, the error in dT (deviation of the analyzed sample temperature from the reference sample temperature) is determined by the error in measuring dR/R .

The principal architecture of the MOCAM-QEPAS sensor for temperature measurements is shown in Fig. 1. Emission of Lasers 1 and 2 is wavelength-modulated with the same frequency f . Then the identically combined emission of the two lasers is directed to two QEPAS cells, one containing the reference gas sample (RGS) and the other the analyzed gas sample (AGS). To enhance the QEPAS signal, and hence increase the trace gas detection sensitivity, the quartz tuning fork (QTF) used in this setup was coupled with an acoustic organ pipe type micro-resonator [12]. The center wavelength of both lasers must be locked to the two respective absorption lines A and B of the target gas (acetylene in our feasibility demonstration). The magnitude of the $2f$ QEPAS signal generated by the radiation of Laser 1 depends on the peak absorption (which is proportional to the gas concentration), the width of the spectroscopic line A, and the output power and WM depth of Laser 1.

Hence, by adjusting the power of Laser 1, P_1 and/or its modulation depth, the corresponding QEPAS signal can be made equal to the signal generated by Laser 2 due to the spectroscopic line B. Now, if at the same time the phase of the WM of Laser 1 is shifted with respect to the WM of Laser 2, then the $2f$ QEPAS signals generated by Lasers 1 and 2 will be opposite in sign and cancel each other. In other words, the two signals in the reference QEPAS cell U_R can

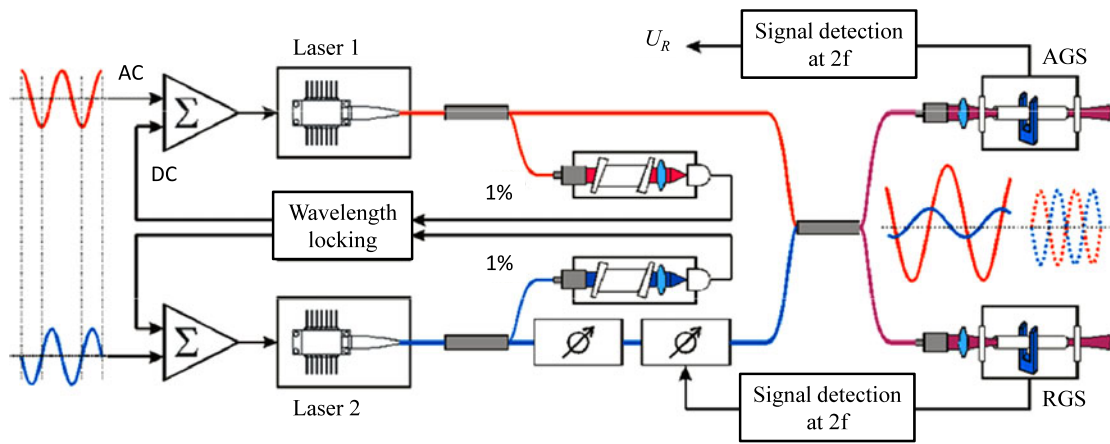


Fig. 1 Principal architecture of the MOCAM-QEPAS sensor configuration for temperature difference measurements in a gas mixture

be balanced in such a way that no sound generation occurs and the transducer (i.e., a quartz tuning fork, QTF, in the case of QEPAS) does not detect any signal with an uncertainty of the QTF thermal noise δ_R , that is,

$$U_R = k_R(P_1 S_1^R - P_2 S_2^R) = 0 \pm \delta_R \tag{6}$$

Here, k_R describes the responsivity of the reference spectrophone, P_1, P_2 are the respective output optical powers of Lasers 1, 2, and S_1, S_2 are the respective line strengths of the two absorption lines A and B. Therefore, we obtain

$$P_2 = P_1 \frac{S_1^R}{S_2^R} \pm \frac{\delta_R}{k_R S_2^R} \tag{7}$$

The signal from the analyzed sample is

$$U = k \left(P_1 S_1 - P_1 \frac{S_1^R}{S_2^R} S_2 \pm \frac{\delta_R}{k_R} \frac{S_2}{S_2^R} \right) \pm \delta$$

$$= k P_1 S_2 \left(\frac{S_1}{S_2} - \frac{S_1^R}{S_2^R} \right) \pm \frac{k}{k_R} \frac{S_2}{S_2^R} \delta_R \pm \delta \tag{8}$$

(variables refer to the analyzed sample and its cell have no upper index). The expression in the last brackets is ΔR . Hence,

$$\Delta R = \frac{1}{k P_1 S_2} \left(U \pm \frac{k}{k_R} \frac{S_2}{S_2^R} \delta_R \pm \delta \right) \tag{9}$$

and

$$\frac{\Delta R}{R} = \frac{1}{k P_1 S_2} \frac{S_2}{S_1} \left(U \pm \frac{k}{k_R} \frac{S_2}{S_2^R} \delta_R \pm \delta \right)$$

$$= \frac{U}{k P_1 S_1} \pm \frac{S_2}{S_2^R} \frac{1}{k_R P_1 S_1} \delta_R \pm \frac{1}{k P_1 S_1} \delta \tag{10}$$

Assuming that the QEPAS spectrophones are similar ($k_R \approx k$ and $\delta_R \approx \delta$) and the temperature difference is small com-

pared to the absolute temperature ($S_2 \approx S_2^R$), we obtain

$$\frac{\Delta R}{R} \approx \frac{1}{k P_1 S_1} (U \pm \delta \sqrt{2}) \tag{11}$$

The temperature difference between two samples will be calculated using the (5). The $\sqrt{2}$ coefficient reflects the fact that the noise of two spectrophones is uncorrelated and, therefore, adds up in quadrature. The coefficient $T^2/\Delta E$ will be included in a constant obtained by means of calibration together with k . $\Delta R/R$ is obtained from (11). Hence, the temperature difference is

$$\Delta T = C \frac{U}{k P_1 S_1} = C \frac{U}{U_1} \tag{12}$$

Here, U is the signal detected from the analyzed sample when the signal from the reference cell is zero (cancelled by balancing the two lasers). $U_1 = k P_1 S_1$ is the signal detected from the analyzed sample when Laser 2 is turned off (or its modulation is disabled).

Based on (11) and using

$$\delta R = \frac{dR}{dT} \delta T \tag{13}$$

where δR is the change in R when the temperature is changed. We can rewrite (11) in the following form:

$$\delta T = \frac{R}{dR/dT} \frac{\delta \sqrt{2}}{k P_1 S_1} = \frac{1}{dR/dT} \frac{\delta \sqrt{2}}{k P_1 S_2} \tag{14}$$

Here, δT represents the uncertainty in the T measurements due to the noise in the photoacoustic signal δ and

$$\frac{\delta}{k P_1 S_1} = \frac{1}{\text{SNR}} \tag{15}$$

where SNR is the signal-to-noise ratio when Laser 2 is blocked. Thus, the larger the factor $dR/dT S_2$ the most accurate are temperature measurements, S_2 refers to the weaker line.

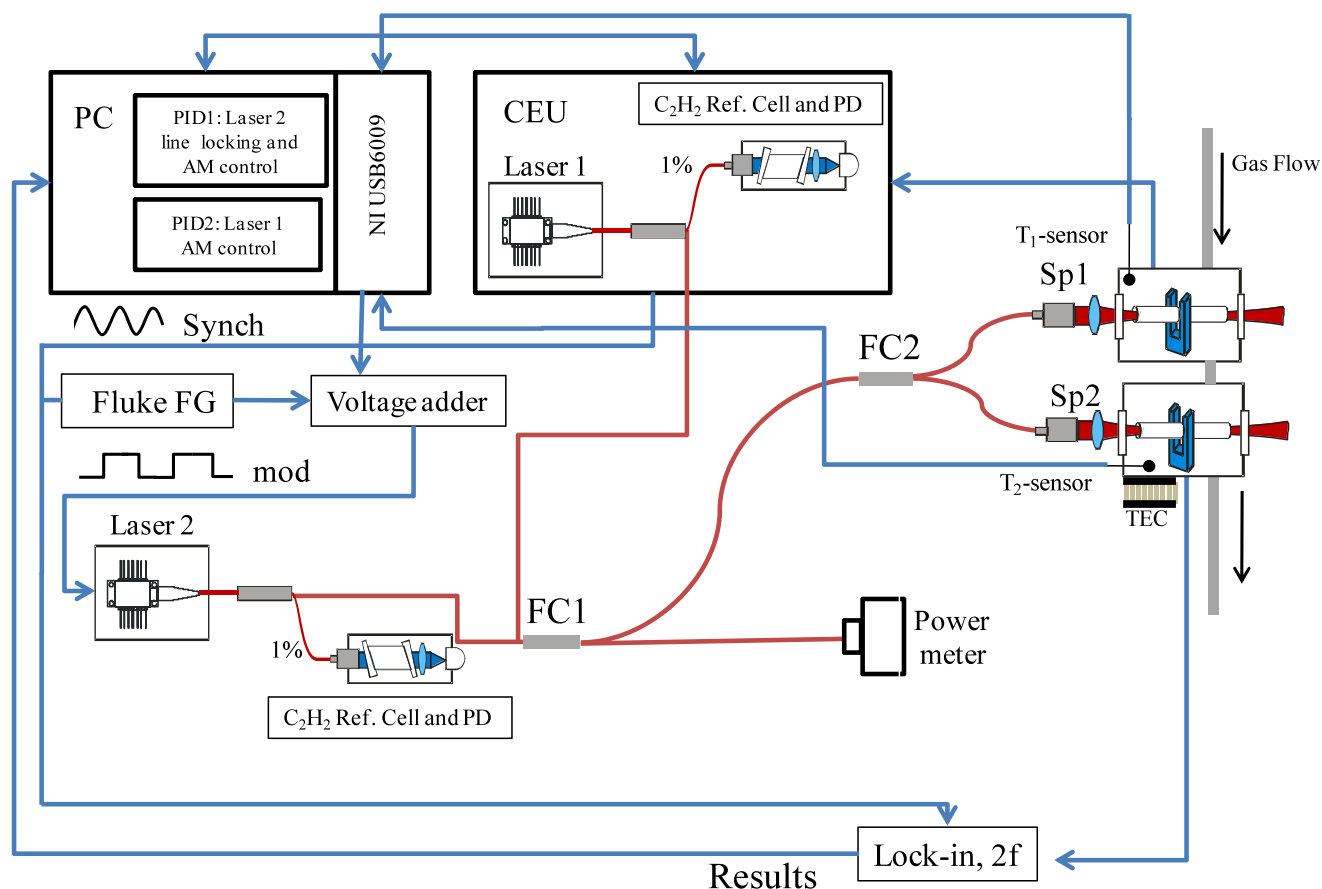


Fig. 2 Schematic of MOCAM-QEPAS setup for small temperature measurements in a gas mixture. *PD*—photodetector; *FG*—function generator; *FC1, 2*—50:50 optical fiber couplers; *Sp1*—QEPAS spectrophone for reference cell; *Sp2*—QEPAS spectrophone for the analy-

sis sample cell; T_1 ; T_2 —Thermistors; *TEC*—thermoelectric cooler. *Blue lines* correspond to electrical connections and *red lines* correspond to fiber optic connections. (*sync*)—synchronization signal from CEU; *mod*—modulation signal for driver of Laser 2

To demonstrate the feasibility of MOCAM for small temperature measurements, we selected an acetylene (C_2H_2)/ N_2 gas mixture with 0.5% C_2H_2 concentration. Based on our inventory of available near-infrared diode lasers, we selected a pair ν_1 , $\nu_2 = 6539.454$, 6529.172 cm^{-1} . For this line pair, $R/(dR/dT) = -689.3^\circ\text{C}$. In Fig. 2, the schematic of the experimental setup is depicted. Two diode lasers (JDS Uniphase) were used. Laser 1 emitted at 6529.17 cm^{-1} . Line locking of Laser 1 was provided by a custom built electronic unit (CEU) by means of an internal reference cell and detector. The $3f$ frequency component of the detector output served as an error signal in the line-locking feedback loop. Laser 2 was locked at 6539.45 cm^{-1} in a similar way by using an additional reference cell and lock-in. For both lasers 1% of the total power was used for line locking by means of two optical fiber splitters. The frequency, amplitude modulation, and voltage for diode Laser 1 was also provided by the CEU; to drive Laser 2 we used a function generator (Fluke model 8150MHz) and the analog output of a USB data acquisition card (National Instrument DAQCard USB6009). A voltage adder was used to sum

the two voltage signals. Both the CEU and the DAQCard USB6009 were controlled by a personal computer which used a Labview program. The two laser beams were combined using 50:50 optical fiber couplers (FC1—OZ Optics model Fused-12-1300/1550-9/125-50/50-3A3A3A-1-0.5). Half of the optical power was used to monitor the laser operation.

Subsequently the optical beam was coupled to an additional 50:50 optical coupler (FC2) and the two final beams were focused through the reference and sample QEPAS cells.

The optical power of Lasers 1 and 2 entering the two QEPAS cells was 16 mW and 14 mW, respectively. Measurements were carried out at atmospheric pressure, with the gas flow set at a constant rate of 100 scc/min. The volume of the two QEPAS cell was $\sim 1.3 \text{ cm}^3$. The temperature of each cell was monitored using a thermistor, which was attached to a wall of the cell. Since the specific heat of the gas is low, thermal equilibrium with the solid walls is quickly reached. Additional thermistors were placed near the gas entrance and exit points of each cell to verify that the gas mixture was

in thermal equilibrium. We varied the temperature of the gas inside the sample cell by using a TEC, while the reference cell was kept fixed at room temperature (RT). Although the two QEPAS spectrophones were designed to be identical, small variation in the tuning fork/micro-resonator mounting leads to two slightly different QTF resonance frequencies. The resonance frequency of the reference spectrophone was 32.755 Hz, while that of the sample spectrophone was 32.743 Hz. The FWHM of the two resonance curves [13] was ~ 12 Hz, so that the two bandwidths overlapped and, therefore, we chose to drive the lasers at half of the average resonant frequency of 32.749 Hz ($f = 16374.5$ Hz), because the laser crosses the absorption line twice per cycle.

Initially, the same temperature (room temperature) was maintained in both QEPAS cells and the modulated light beam of Laser 2 was phase-shifted in order to achieve a balanced condition. If the conditions in the two cells and the response of the two QEPAS spectrophones were identical, we should have obtained a noise level signal from both of them, but due to the wavelength selectivity of the fiber coupler FC2, we observed a noise level signal in one of the cell and a residual signal in the other. The unbalance was $\sim 3\%$ of the full Laser 1-induced signal. Therefore, we readjusted the modulation index to make the signal in the analyzed sample cell zero when $\Delta T = 0$. This procedure resulted in a nonzero signal in the reference cell, and a computer-controlled feedback loop was set to keep this signal at constant level. The advantage of maintaining this offset with a feedback loop, over subtracting the residual signal observed for $\Delta r/r$, was that we could set a higher sensitivity for the lock-in amplifier connected with the sample cell. If an offset had occurred, we would have had to reserve sufficient dynamic range for the lock-in channel, otherwise the channel would have been saturated by the offset. However, a large dynamic range means lower signal sensitivity.

The analyzed sample cell temperature was varied between 20°C to 40°C. By measuring the corresponding signals U_1 and U (obtained by turning off the modulation of Laser 2 and using (12) we extracted the calibration constant $C = 403.6$ K. To evaluate the MOCAM-QEPAS precision as a temperature sensor, we adjusted the gas temperature in the sample cell, by using the corresponding TEC and compared the temperature difference between the two cells as measured by the two thermistors with that determined by MOCAM based QEPAS. The results are plotted in Fig. 3, confirming linearity of MOCAM measurements.

To determine the sensitivity of the MOCAM-QEPAS sensor we performed an Allan variance analysis while keeping the temperature identical in both reference and sample cells. The lowest error was obtained for an integration time of 17 sec (i.e., 0.046 Hz bandwidth), and corresponded to a sensitivity of 30 mK or 140 mK/Hz $^{1/2}$. The expected sensitivity can be extracted from (14) and the coefficient $\frac{8\sqrt{2}}{kP_1A_1}$

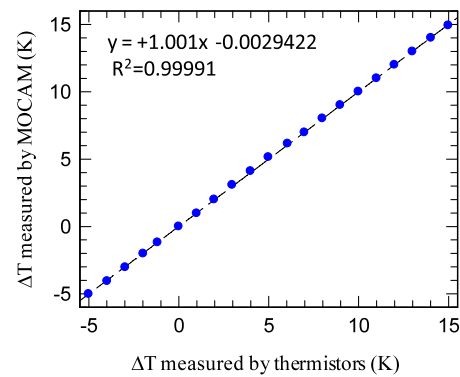


Fig. 3 Comparison of the temperature differences between sample and reference QEPAS cells measured by using the two thermistors $T_{1,2}$ with those extracted by MOCAM-QEPAS. The black dashed line is a linear fit of the data

in our performance evaluation was 2.5×10^{-5} Hz $^{-1/2}$. We obtained a sensitivity of 17 mK/Hz $^{1/2}$. The observed excess noise was due to laser power fluctuations and the non-optimal sensor configuration, since the signal in the reference cell was not zero and is ~ 8 times greater than the thermal noise for the 0.0785 Hz bandwidth. This limit can be improved by using more stable lasers in terms of optical power and wavelength and by exactly balancing the reference cell, perhaps by inserting attenuators in the optical path of one of the two lasers.

2 MOCAM for detection of broadband molecular absorbers

Vibrational spectra of most molecules consisting of more than five atoms are so dense that Doppler and pressure broadening make them unresolved at normal temperature and pressure conditions. As a result, infrared absorption spectra of such polyatomic molecules consist of quasi-unstructured bands, each 100–200 cm $^{-1}$ wide. Spectroscopic identification of these species requires optical sources with wide spectral coverage, and the use of DFB or FP semiconductor lasers for this purpose is problematic, since they usually cannot be wavelength modulated with sufficient spectral tuning to cover the absorption feature. Thus, QEPAS detection of such molecules would require AM of the laser radiation. In this case, the scattered and subsequently absorbed light will create a coherent background, making sensitive concentration measurements difficult.

The schematic of the MOCAM QEPAS sensor configuration that we propose for the sensing of broadband molecular absorbers is shown in Fig. 4. It refers to the detection of a target species A with broad unresolved absorption features. The idea is to have two excitation sources, with the wavelength of the first one centered on the target absorption feature, while the second source is tuned to the background

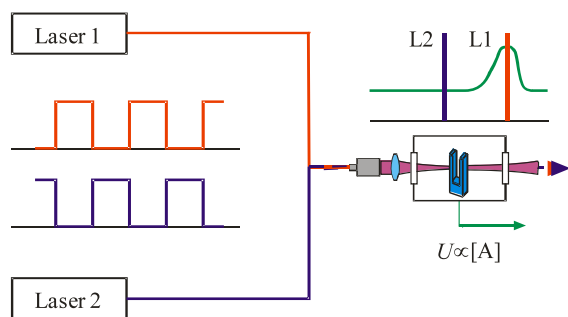


Fig. 4 MOCAM applied to the detection of broadband absorbers such as polyatomic molecules or aerosols. U is the signal measured from the QEPAS cell and $[A]$ is the gas target concentration

spectral region. When the two lasers are AM modulated with a 180° phase shift, the modulation amplitudes can be adjusted so that there is no AC signal U in the absence of A . If the concentration, $[A] \neq 0$, the detected signal at the modulation frequency is proportional to it. Figure 4 shows rectangular AM, but it can be any waveform with a 50% duty cycle.

In order to demonstrate the feasibility of a MOCAM based QEPAS for the efficient detection of large molecular absorbers, we selected hydrazine (N_2H_4) vapor. N_2H_4 is a highly toxic, unstable, and strongly corrosive gas that is used in polymer production, the pharmaceutical industry and as a rocket fuel. NASA seeks to avoid contamination of the Space Station environment, and so N_2H_4 must be detected at part per billion (ppb) concentration levels after astronauts perform EVA tasks. Two commercial wide stripe Fabry–Perot diode lasers (Laser 1: high power $100\ \mu\text{m}$ stripe lasers, Princeton Lightwave; Laser 2: NL-C-1.5-1566, nLight) with emissions centered at $\sim 6370\ \text{cm}^{-1}$ and $6570\ \text{cm}^{-1}$ on the tail and on the peak of the hydrazine absorption band, respectively. The spectral positions of the diode lasers used in this work are shown in Fig. 5 along with the hydrazine vapor absorption spectrum from the Pacific Northwest National Laboratory (PNNL) spectral database. The plot depicts data points corresponding to different laser temperatures with a fixed injection current of 2 A. In our experiments, the operating temperature was set to 28°C for Laser 1 and to 18°C for Laser 2. The spectral width of each laser was $\sim 40\ \text{cm}^{-1}$. Wide stripe diode lasers can deliver high optical power levels that exceed 1 W. Such diode lasers are usually not used for spectroscopic applications because they typically exhibit high divergence and multimode (both spatially and spectrally) behavior. Therefore, since it is impossible to shape a narrow, low divergence beam, there is no way to efficiently couple the radiation from a wide stripe laser into a multipass cell or an optical cavity. However, QEPAS [8, 9] offers a promising sensor platform for broadband molecular absorbers, using wide stripe semiconductor lasers. This is possible because QTFs are wavelength insensitive transducers with a very short optical path length (0.3 mm).

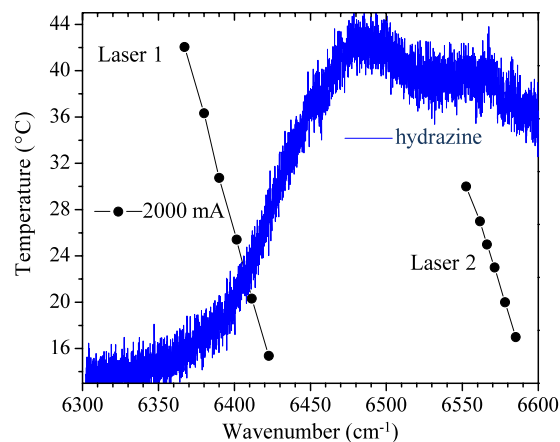


Fig. 5 Spectral position of the two wide stripe diode lasers with respect to near-infrared hydrazine absorption band (blue line, PNNL database), as a function of the operating temperature and at a fixed injected current of 2 A

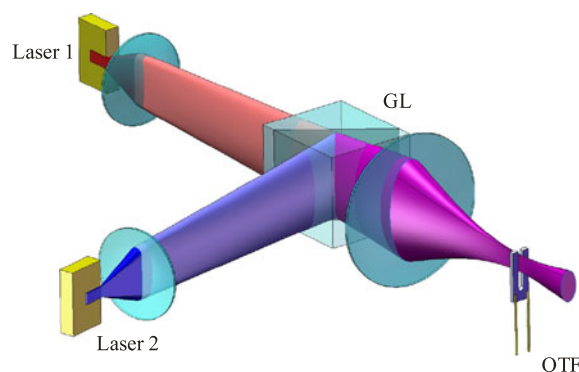


Fig. 6 Optical setup of the MOCAM-QEPAS based hydrazine sensor. Laser 1, 2—wide stripe lasers; GL—Glan prism; QTF—quartz tuning fork

The schematic of the optical system used for the detection of broadband molecular absorbers is shown in Fig. 6. In contrast to most QEPAS sensors, an acoustic microresonator was not used, thus reducing the probed optical path to the QTF thickness, 0.3 mm. The optical system was designed to produce a magnified image of the $100\ \mu\text{m}$ wide laser facet in the $0.3 \times 0.3 \times 3.6\ \text{mm}^3$ gas volume between the prongs of a QTF. In practice, it is not possible to completely avoid irradiating the QTF with stray laser radiation, which results in an unwanted background signal that is not related to optical absorption in the gas to be analyzed.

In order to suppress the unwanted background, we exploited the MOCAM method. Both Lasers 1 and 2 emit linearly polarized light. The polarization plane of one of the lasers was rotated 90° by means of half-wavelength plate (not shown in Fig. 6). The radiation emitted by the two lasers was combined using the Glan polarizer, GL. The overlapped images of the laser facets were located between the QTF prongs. Injection currents of the two lasers were mod-

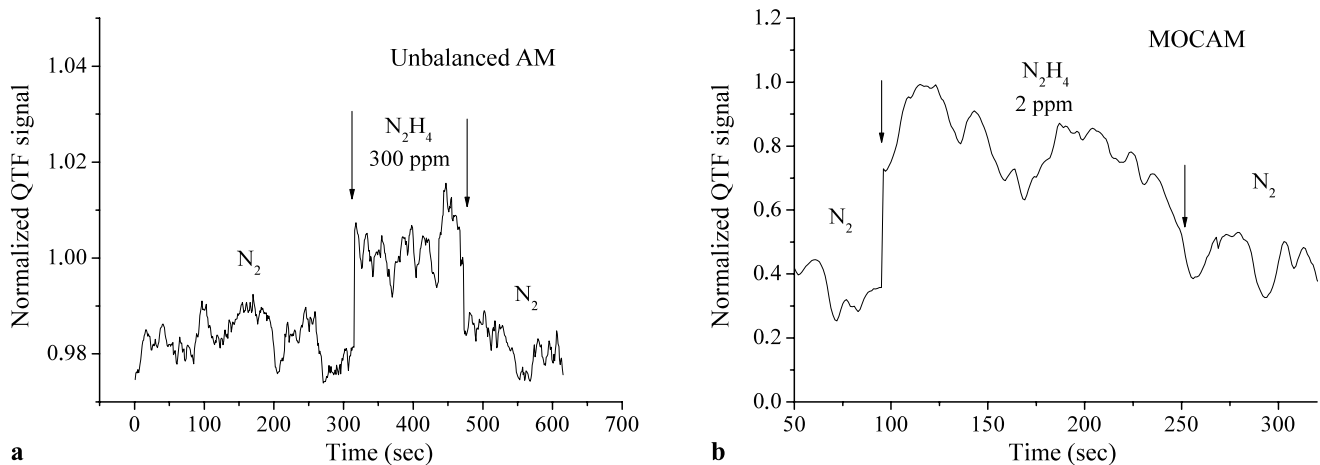


Fig. 7 Comparison between unbalanced AM (a) and MOCAM (b), for a gas sample with a concentration of 300 ppm and 2 ppm of hydrazine, respectively. The arrows indicate the turn-on and turn-off of hydrazine: N_2 flux inside the QTF spectrophone

ulated from threshold to an adjustable maximum value using sinusoidal waveforms with a 180° phase shift. The intensities were balanced so that the acoustic signal induced by spectrally nonselective absorption of stray radiation was cancelled. The resulting signal was proportional to the spectrally selective optical absorption of the chemical species A. The gas pressure was set at 700 torr. The optical power of L1 and L2 passing through the tuning fork prongs were 122 mW and 62 mW, respectively. Figure 7 depicts a comparison between two representative hydrazine concentration measurements. Figure 7a shows a standard AM detection scheme with a sample of 300 part per million (ppm) of hydrazine in N_2 , and the observed signal of only $\sim 2\%$ above the background. Figure 7b shows a 2 ppm concentration of hydrazine in N_2 being detected using the MOCAM method, and the signal is more than 4 times higher than the background. Thus, the MOCAM technique suppressed the background signal level by approximately three orders of magnitude as compared to unbalanced (one laser) detection. The hydrazine vapor detection limit was ~ 1 ppm with a 1 sec averaging time, corresponding to a $k \sim 1.4 \times 10^{-7} \text{ cm}^{-1}$, or 4.1×10^{-9} fractional absorption in the probed 0.3 mm path length. Noise suppression and sensitivity did not improve in balanced detection mode and was laser-dominated, ~ 100 times higher than the QTF thermal noise limit. Better spatial filtering of the laser radiation and active balancing of the diode lasers is needed to improve the SNR and approach the QTF thermal noise limit.

3 Conclusions

In summary, the feasibility of a novel spectroscopic technique, MOCAM, combined with QEPAS, was demonstrated for temperature difference measurements and for the detection of a broadband molecular absorber (e.g., hydrazine).

We demonstrated that two lasers can be modulated in such a way that they cancel each other's background signal. For both applications of MOCAM, noise and detection sensitivity were laser-dominated and higher than the QTF thermal noise limit. Hence, to achieve a sensitivity sufficient for isotopic measurements, radiation filtering and active balancing of the two lasers must be improved. Finally, since the MOCAM technique yields a signal proportional to the deviation from a balanced system state, a further application can be the design of a controller that uses a MOCAM signal to drive a feedback loop to control critical parameters in manufacturing processes requiring precise mixing of chemical components.

Acknowledgements The Rice University group acknowledges financial support from a National Science Foundation ERC MIRTHE award and a grant C-0586 from The Welch Foundation. V. Spagnolo acknowledges financial support from the Regione Puglia "Intervento Cod. DM01, Progetti di ricerca industriale connessi con la strategia realizzativa elaborata dal Distretto Tecnologico della Meccatronica."

References

1. A.A. Kosterev, R.F. Curl, Int. Patent WO 2007/056772 A2, 2007
2. V. Spagnolo, L. Dong, A.A. Kosterev, D. Thomazy, J.H. Doty, F.K. Tittel, Opt. Lett. **36**, 460 (2011)
3. A. Castrillo, G. Casa, E. Kerstel, L. Gianfrani, Appl. Phys. B **81**, 863 (2005)
4. H. Wächter, J. Mohn, B. Tuzson, L. Emmenegger, M.W. Sigrist, Opt. Express **16**, 9239 (2008)
5. J.B. McManus, D.D. Nelson, J.H. Shorter, R. Jimenez, S. Herndon, S. Saleska, M. Zahniser, J. Mod. Opt. **52**, 2309 (2005)
6. J.A. Silver, D.J. Kane, Meas. Sci. Technol. **10**, 845 (1999)
7. R. Lewicki, G. Wysocki, A.A. Kosterev, F.K. Tittel, Opt. Express **15**, 7357 (2007)
8. A.A. Kosterev, Y.A. Bakhirkin, R.F. Curl, F.K. Tittel, Opt. Lett. **27**, 1902 (2002)
9. A.A. Kosterev, F.K. Tittel, D. Serebryakov, A.L. Malinovsky, I. Morozov, Rev. Sci. Instrum. **76**, 1 (2005)

10. J.A. Silver, D.J. Kane, *Meas. Sci. Technol.* **10**, 845 (1999)
11. G. Herzberg, *Molecular Spectra and Molecular Structure II. Spectra of Diatomic Molecules* (Van Nostrand Reinhold, New York, 1950)
12. L. Dong, A.A. Kosterev, D. Thomazy, F.K. Tittel, *Appl. Phys. B* **100**, 627 (2010)
13. N. Petra, J. Zweck, A.A. Kosterev, S.E. Minkoff, D. Thomazy, *Appl. Phys. B* **94**, 673 (2009)